Research Square

Preprints are preliminary reports that have not undergone peer review.
They should not be considered conclusive, used to inform clinical practice,
or referenced by the media as validated information.

Flooding stress affects microsporogenesis, anther development, and pollen quality in tomato (Solanum lycopersicum L.)

Yanina de Jesús Pérez
Instituto de Botánica del Nordeste
Lucía Melisa Zini
Instituto de Botánica del Nordeste
Francesco Mignolli
Instituto de Botánica del Nordeste
Silvia Schaller
Instituto de Botánica del Nordeste
Ana María Gonzalez
Instituto de Botánica del Nordeste
María Laura Vidoz
mlvidoz@agr.unne.edu.ar

Instituto de Botánica del Nordeste

Research Article

Keywords: microsporogenesis, cytogenetics, flooding, global warming, abiotic stress, tomato

Posted Date: November 4th, 2026

DOI: https://doi.org/10.21203/rs.3.rs-11192489/v1

License: This work is licensed under a Creative Commons Attribution 4.0 International License.
Read Full License

Additional Declarations: No competing interests reported.

Flooding stress affects microsporogenesis, anther development, and pollen quality in tomato (*Solanum lycopersicum* L.)

Authors: Yanina de Jesús Pérez[a, c, i]; Lucía Melisa Zini[a, b, d]; Francesco Mignolli[a, b, e]; Silvia Schaller[a, f]; Ana María Gonzalez[a, b, g]; María Laura Vidoz[a, b, h, i]

[a] Instituto de Botánica del Nordeste, Consejo Nacional de Investigaciones Científicas y Técnicas, Universidad Nacional del Nordeste, Sargento Cabral 2131, 3400, Corrientes, Argentina.

[b] Facultad de Ciencias Agrarias, Universidad Nacional del Nordeste, Sargento Cabral 2131, 3400, Corrientes, Argentina.

[c] https://orcid.org/0000-0003-3181-0391

[d] https://orcid.org/0000-0001-5154-1112

[e]https://orcid.org/0000-0003-1346-6734

[f] https://orcid.org/0000-0002-2548-2814

[g] https://orcid.org/0000-0002-9311-0967

[h] https://orcid.org/0000-0001-8290-8538

[i] Correspondig authors: Yanina de Jesús Pérez; María Laura Vidoz

Abstract
Flooding is an increasing threat to crop productivity under climate change, affecting the reproductive development of many crop plants. Although flooding effects on tomato physiology, growth, and yield are well documented, its impact on male reproductive development remains poorly understood. Here, we investigated the effects of flooding on male gametophyte development in tomato (*Solanum lycopersicum* L. cv. Ailsa Craig) using cytogenetic, histological, and pollen performance analyses. Compared with controls, flooded plants showed a higher proportion of meiocytes at later stages, particularly during meiosis II. Meiotic asynchrony was the meiotic irregularity with higher frequency, and trinuclear configurations at telophase II increased significantly. Flooding was also associated with a significant increase in triads, indicating altered sporad formation. Histological analyses of anther development revealed alterations at specific floral stages, including degeneration of microspore mother cells and abnormal tapetal morphology. *In vitro* pollen germination was reduced. Overall, six-days of flooding did not cause total male sterility but were associated with alterations in male reproductive development, from meiosis through pollen maturation. These findings identify male reproductive development as a sensitive target of flooding stress and provide new insights into the vulnerable developmental stages in tomato. Understanding these responses may support the development of management strategies and breeding approaches aimed at improving reproductive resilience under increasingly variable water regimes associated with climate change.

Key words: microsporogenesis, cytogenetics, flooding, global warming, abiotic stress, tomato

Introduction

The reproductive stage of flowering plants is particularly vulnerable to abiotic stressors, including fluctuations in water availability, humidity, nutrient composition and temperature (Zhang et al. 2025). Deviations from optimal conditions during gamete development, stigma receptivity, pollination, and fertilisation can reduce reproductive success and negatively affect crop productivity (Choudhary et al. 2022; Resentini et al. 2023; Begcy et al. 2024). Climate change is increasing the frequency and intensity of heat waves, drought periods, water scarcity, flooding, polar ice melting, and biodiversity loss (Qian et al. 2025). These accelerated environmental shifts are seriously threatening agricultural productivity, particularly affecting crop yield and quality, driving land-use change, and promoting the development of new strategies to mitigate the impacts on food availability.

Adverse environmental conditions during reproductive development frequently impair pollen viability, reduce fertilisation success, and decrease fruit quality and seed set. Male gamete development is particularly sensitive to environmental stress: high temperature can disrupt meiotic progression and pollen development in tomato (Schindfessel et al. 2023), while waterlogging has been shown to impair pollen fertility through alterations in anther carbohydrate and antioxidant metabolism in other crop species (Huang et al. 2023). However, the effects of flooding on microsporogenesis and anther development in tomato remain poorly understood. Understanding male gamete development under environmental stress is essential for identifying vulnerable stages and designing strategies to improve crop resilience and stabilise yield (Ganie and Foyer 2023).

Physiological studies in tomato plants (*Solanum lycopersicum* L.) have demonstrated that the root system is highly sensitive to flooding stress (Vidoz et al. 2010; Mignolli et al. 2020, 2021). Under

hypoxic conditions, roots rapidly lose their ability to conduct water, and their respiration rate decreases, leading to fermentative metabolism, reactive oxygen species accumulation, and cytoplasmic acidification, which can ultimately cause root damage and death (Germain et al. 1997; Safavi-Rizi et al. 2020; Mignolli et al. 2021). Prolonged exposure to flooding also affects shoot performance, causing earlier leaf senescence, reduced growth, decreased leaf expansion, and lower photosynthetic activity and photochemical efficiency (Horchani et al. 2008; Vidoz et al. 2016; De Pedro et al. 2020).

Most studies on tomato flooding stress have focused on physiological responses, metabolic changes, and the identification of genes and hormones involved in tolerance or injury (Jackson and Campbell 1976; Germain et al. 1997; Horchani et al. 2008; Else et al. 2009; Vidoz et al. 2010, 2016; Mignolli et al. 2020, 2021; Yin et al. 2023). In contrast, research on the reproductive phase has largely concentrated on fruit development and yield-related traits (Ezin et al. 2010; Horchani et al. 2008, 2011; Horchani and Aschi-Smiti 2011). These studies quantified flower buds, flowers, and fruits after flooding (Horchani et al. 2008), measured fruit number, weight, and size under hypoxia (Ezin et al. 2010), and analysed biochemical and hormonal changes during fruit development (Horchani et al. 2011; Horchani and Aschi-Smiti 2011), showing that hypoxia markedly affects reproductive performance. Nevertheless, the effects on earlier reproductive stages remain poorly understood, which is a fundamental gap because gametogenesis is highly sensitive to environmental perturbations, and its disruption may compromise fertilisation. Heat stress in tomato can reduce pollen viability and germination (Jegadeesan et al. 2018) and disrupt tapetal and microspore development (Giorno et al. 2013), while drought can induce abnormal anther and pollen development, with the tetrad-to-vacuolated uninucleate microspore stages being particularly sensitive (Lamin-Samu et al. 2021). Waterlogging has also been shown to reduce pollen fertility in cotton (Huang et al. 2023), but its effects on microsporogenesis and anther development in tomato remain poorly characterised.

The cultivated tomato is a well-established model for cytogenetic and meiotic studies because of its characterised genome and meiotic behaviour (Rick and Butler, 1956; Nikolova et al. 2008; Peters and Underwood 2023). Cytological analyses can therefore reveal stress-induced defects in homolog pairing, recombination, and chromosome segregation; in tomato, heat stress has been shown to impair synapsis, chiasma formation, and meiotic chromosome segregation (Schindfessel et al. 2023). Whether flooding similarly affects meiotic progression in tomato remains unclear.

Given that root hypoxia constrains growth and reproduction in tomato, this study integrated cytogenetic and embryological approaches to improve our understanding of how male development and pollen formation are affected. We assessed the effects of flooding with the following aims: (1) to analyse meiotic behaviour in flooded and non-flooded plants; (2) to evaluate the histological responses of anthers during pre-pollination stages under flooding; and (3) to estimate pollen quality produced under both experimental conditions. This knowledge improves our understanding of tomato reproductive development under stress and is necessary to identify vulnerable floral stages associated with tomato yield losses.

Materials and methods

Plant material and growth conditions

The study was conducted on *Solanum lycopersicum* cv. Ailsa Craig (AC; accession LA2838A). This cultivar was developed in the United Kingdom in the early 20th century (Darby et al. 1978; Kouchnareva 2017). AC is an indeterminate tomato cultivar that produces medium-sized, round red fruits and has been widely used as a wild-type reference genotype in physiological, genetic, and mutant studies of tomato stress biology (Beisken et al. 2014; Vidoz et al. 2010, 2016; Mignolli et al. 2020). Seeds obtained from the Tomato Genetics Resource Center (TGRC, University of California, Davis), were first sown in plastic trays (Fig. 1 a, b) and then transplanted to 1 L plastic pots. Seedlings and plants were grown in climate chambers (26 ± 2 °C, 50–70% relative humidity, 16 h light per day and a light intensity of 200 μmol m^{-2} s^{-1}) and regularly watered.

Flooding treatment, material collection and fixation

Six weeks after sowing, when the first flowers of the inflorescences were fully open, the flooding treatment was imposed according to De Pedro et al. (2020). Twenty eight plants, each growing in an individual 1 L pot, were used. Half of the pots were subjected to flooding, with the water level maintained at the cotyledons. The remaining fourteen pots were placed in a separate tank, watered regularly, and allowed to drain freely (Fig. 1c, d). The experiment was performed between April and May 2026. Inflorescences containing flowers at different developmental stages were labelled. After 6 days of flooding treatment, floral buds and flowers were collected (Fig. 1d).

Floral development stages were defined based on flower length, measured as the distance from the receptacle to the sepal apex at the end of the flooding treatment (Fig. 1e). Samples were fixed in FAA (formaldehyde: acetic acid: ethanol, 5:5:90 v/v) and lactic acid-ethanol solution (1:5 v/v; Fernández 1973) and subsequently stored in 70% ethanol at 4 °C.

Analysis of meiosis and tetrads

Anthers containing microspore mother cells (MMCs) and tetrads, previously fixed in a lactic acid-ethanol solution, were squashed and stained with 2% lactopropionic orcein, as described by Dyer (1963). A total of ten slides per treatment were analysed. Meiotic analysis included the assessment of meiotic behaviour in microspore mother cells (MMCs) at prophase I (PI), metaphase I (MI), anaphase I (AI), telophase I (TI), prophase II (PII), metaphase II (MII), anaphase II (AII), and telophase II (TII). Tetrads consisting of four equally sized microspores were considered normal. To quantitatively summarize the distribution of meiocytes across successive meiotic stages, a weighted mean meiotic stage (WMMS) was calculated separately for meiosis I and meiosis II. The use of a weighted average of meiotic-stage frequencies to characterize the mean developmental position of pollen mother cell populations has

precedent in plant cytogenetic analyses (Neijzing and Viegas, 1979), although the scoring system used here was specifically defined for the present study. In the present study, successive cytological stages were treated as ordered states and assigned ordinal scores. For meiosis I, prophase I (PI), metaphase I (MI), anaphase I (AI), and telophase I (TI) were assigned scores of 1, 2, 3, and 4, respectively, and the weighted mean meiotic stage for meiosis I (WMMS-I) was calculated as:

$$WMMS\text{-}I = [1(PI) + 2(MI) + 3(AI) + 4(TI)] / (PI + MI + AI + TI)$$

Similarly, prophase II (PII), metaphase II (MII), anaphase II (AII), and telophase II (TII) were assigned scores of 1, 2, 3, and 4, respectively, and the weighted mean meiotic stage for meiosis II (WMMS-II) was calculated as:

$$WMMS\text{-}II = [1(PII) + 2(MII) + 3(AII) + 4(TII)] / (PII + MII + AII + TII)$$

WMMS values range from 1 to 4, with higher values indicating a meiocyte population shifted toward later stages of the respective meiotic division. Because the assigned scores represent ordered cytological categories rather than equivalent temporal intervals, WMMS was interpreted as a summary of meiotic stage distribution rather than as a direct measure of meiotic rate or duration. WMMS-I and WMMS-II were calculated independently for each plant from the raw cell counts, with individual plants considered biological replicates (n = 5 per treatment). Control and flooded plants were compared using an exact one-sided Mann–Whitney U test.

Anther development

Control and 6-day flooded plants were sampled across eight sequential flower developmental stages with five biological replicates per treatment and stage to conduct a chronological comparative analysis of root hypoxia effects on anther tissue histology and pollen development. Flower buds and open flowers fixed in FAA were dehydrated using Biopur® (Rosario, Argentina) histological dehydrant series (Gonzalez and Cristóbal 1997). Paraffin infiltration followed the technique of Johansen (1940). Flowers were embedded in Histowax (Biopack, Buenos Aires, Argentina) and transversely and longitudinally sectioned at 10-12 μm using a rotary microtome (MICROM, Walldorf, Germany). The sections were stained with a combination of safranin and Astra blue (Luque et al. 1996) and were mounted with synthetic Canada balsam.

Pollen stainability and germination tests

For pollen stainability and germination tests, we used flowers and each individual plant served as independent biological replicates (n = 10 plants per treatment). From each plant, one flower with mature anthers was sampled. Pollen viability was estimated indirectly using carmine:glycerine staining (1:1) according to Pittenger and Frolik (1951). Between 775 to 1600 pollen grains per flower were examined,

and pollen grains exhibiting uniform and intense staining were considered viable, whereas those with weak or no staining were classified as non-viable. The percentage of viable pollen was estimated by dividing the number of coloured pollen grains by the total number of pollen grains and multiplying by 100.

To test *in vitro* pollen germination, pollen samples were germinated on a modified Brewbaker and Kwack (1963) medium containing 0.35% agar, 10% sucrose, 100 ppm H_3BO_3, 100 ppm $MgSO_4H_2O$, and 100 ppm KNO3 at pH 5.2. Pollen grains were uniformly spread over the microscope slides with two drops of germination medium and then placed in a Petri dish. Moistened absorbent tissue paper was placed under the slide to maintain humidity. Samples were incubated in darkness in a growth chamber at 27 °C. After three hours of incubation, the samples were fixed with 2% lactopropionic orcein and covered with a coverslip. Pollen grains were scored as germinated when the pollen tube length exceeded twice the pollen diameter. Ten slides per treatment were examined, and approximately 800 pollen grains were scored for each sample.

Histological sections, meiotic preparations, and pollen samples were examined and photographed using a light microscope (Leica DM LB2, Wetzlar, Germany) equipped with a Leica ICC50 HD digital camera.

Statistical analysis

Data are presented as means ± SEM. Normality and homoscedasticity were assessed using Shapiro-Wilk and Levene's tests, respectively. Depending on data distribution and variance homogeneity, control and flooded plants were compared using Student's t-test, Welch's t-test, or the Mann-Whitney U test. Meiotic progression indices were compared using exact one-sided Mann-Whitney tests. Statistical significance was set at $p < 0.05$.

Results

This study included the developmental histology of anthers and all observable stages of male gamete formation: the microspore mother cell (MMC) stage, meiosis (including chromosome behaviour), tetrad formation, and pollen maturation and fertility. The latter was evaluated by pollen stainability and in vitro pollen germination tests.

Meiosis in tomato

Meiosis I and II in control and flooded plants displayed meiotic abnormalities (Fig. 2 a–o). The distribution of meiotic phases varied between treatments: control plants showed a higher proportion of cells in prophase I, whereas flooded plants showed a higher proportion in telophase II (Fig. 2p). This shift towards later meiotic stages in flooded plants was noteworthy. Indeed, WMMS showed that flooding shifted the distribution of meiocytes towards later stages in both meiotic divisions (Table 1). The WMMS-I increased from 1.60 ± 0.14 in control plants to 1.99 ± 0.21 under flooding. A more

pronounced response was observed during meiosis II, where the WMMS-II increased from 1.77 ± 0.31 to 2.85 ± 0.34. Both differences were significant, indicating that meiotic progression was more advanced in flooded plants, particularly during meiosis II.

The rate of meiotic aberrations remained moderately low in control plants (Fig. 2q). Abnormalities such as lagging chromosomes (metaphase I and II, anaphase I, and late telophase I; Fig. 2d, f, g, l), chromosome bridges (anaphase I and II; Fig. 2e, n), and meiotic asynchrony (metaphase II and anaphase II; Fig. 2k–m) displayed slight upward trends under flooding, but none reached statistical significance. Meiotic asynchrony, defined by the co-occurrence of nuclei at different meiotic stages within a single MMC, predominated among meiotic abnormalities in both control and flooded plants, reaching its highest frequency under flooding conditions. This result is consistent with the statistically significant increase in trinuclear cells at telophase II (TII trinuclear).

Microspore tetrad formation

Quantification of post-meiotic sporads revealed that flooding stress significantly altered normal tetrad formation (Fig. 3a). Under control conditions, the vast majority of microsporocytes produced normal tetrads (98.22±0.13%, Fig. 3a–b). Flooding stress caused a statistically significant reduction in the proportion of normal tetrads down to 94.43±0.71% ($p<0.01$). This decline was primarily driven by a significant increase in triads (Fig. 3c), which rose from 1.65±0.12% in controls to 5.44±0.74% in flooded plants ($p<0.01$). Other configurations observed, such as dyads and monads (Fig. 3d–e), occurred at low frequencies (<0.1%) and showed no significant differences between treatments ($p>0.05$).

Histological analysis of anther and pollen development

Histological differences between treatments were observed at several floral stages, particularly in MMC integrity, tapetal morphology, and the developmental stage of microspores and pollen at comparable bud sizes. At the 3 mm floral bud stage (Fig. 4), MMCs were enclosed by anther wall layers consisting of the epidermis with developing trichomes, endothecium, multiseriate middle layer thickened on the dorsal side of the anther, and a vacuolating tapetum. The anther typically comprised four locules separated by two septa, each featuring a parenchymatous placentoid lined by the tapetum (Fig. 4a–b). Two or three rows of MMCs were distinguished by their polyhedral shape, dense cytoplasm, and large nucleus with a prominent nucleolus (Fig. 4b). In the flooding treatment, some developing locules exhibited MMC degeneration. Furthermore, tapetal cells within these locular compartments were abnormally enlarged and vacuolated, indicating precocious tissue degradation (Fig. 4c–d).

At the 4 mm floral bud stage, in both treatments the trichomes in the epidermis and tapetal cells became conspicuous (Fig. 4e, g). As MMCs further differentiated, they became enveloped by a thickened callose wall strongly stained with Astra blue, while their protoplasts became progressively spherical (Fig. 4e–h). Anthers under control conditions possessed locules lined with a secretory tapetum, characterized by binucleate cells with dense cytoplasm and prominent vacuoles (Fig. 4f). In contrast, anthers under

flooding displayed a mixture of normal and aberrant pollen sacs; the latter exhibited early tapetal degradation (Fig. 4g–h).

In 5 mm control flower buds, the anthers spanned the MMC, meiosis, and microspore tetrad stages (Fig. 5a, b, e, f). Tapetal cells at the parietal position reached maximum enlargement prior to meiosis and subsequently underwent volume reduction during tetrad formation, consistent with the normal progression of tapetal degeneration (Fig. 5a, b, e, f). Conversely, the anthers in the flooding treatment showed tapetal degeneration as early as the MMC stage, with tapetal cells characterised by shrunken protoplasts (Fig. 5c–d). At the same bud size, control anthers contained MMCs or tetrads (Fig. 5b, f), whereas flooded anthers also contained free microspores (Fig. 5g–h). The presence of free microspores was accompanied by tapetal hypertrophy, suggesting delayed or disrupted tapetal degeneration (Fig. 5h). In both treatments, successive post-meiotic stages revealed progressive retraction of the parenchymatous tissue forming the placentoids and septa, and this degradation was frequently asynchronous within individual anthers (Fig. 5e, h).

Anthers from 6 mm flower buds contained irregularly shaped microspores at an early stage of vacuolation and degrading tapetal cells. No distinct histological differences were found between the treatments (Fig. 6a–b). By the 7 mm floral bud stage, microgametogenesis had transitioned to the late-vacuolate microspore stage, in which a large central vacuole displaced the single nucleus to the periphery (Fig. 6c–g). In both treatments, pollen apertures developed; endothecial cells enlarged but lacked fibrous thickenings; and tapetal cells exhibited extensive vacuolation alongside complete cytoplasmic breakdown (Fig. 6d–h). At the 7 mm bud stage, control anthers contained predominantly vacuolated uninucleate microspores, whereas flooded anthers contained bicellular pollen. Following pollen mitosis I, standard-sized grains and abnormally large pollen grains or macrograins were identified (Fig. 6g–h). Both types contained a smaller generative nucleus and a larger vegetative nucleus (Fig. 6h).

At the 8 mm floral stage, vacuolated microspores were still present in control anthers. Eventually, they underwent pollen mitosis I to form immature bicellular pollen grains (Fig. 7a–b). In the flooding treatment, the anthers contained young bicellular pollen grains, and standard-sized and macrograins were also identified (Fig. 7c–d). In both treatments, tapetal degeneration was completed during this stage, leaving only tapetal membrane remnants and orbicules (Fig. 7a–d). Between the 8 and 9 mm floral bud stages, the crystal-containing septum had broken down, merging the two microsporangia within each theca into a single locule (Fig. 7e–f). Concomitantly, the one- to two-layered endothecium, which was markedly enlarged in the distal third of the anther and near the stomium, developed lignified wall thickenings (Fig. 7e–f). Pollen grains in both treatments began accumulating nutrient reserves, and the septum lysis was completed (Fig. 7g–h). Anther dehiscence occurred at the late floral stages (10 mm or larger) and during anthesis in both treatments (Fig. 7i–j). After dehiscence, the epidermis, endothecium, and part of the middle layers remained turgid except on the lateral sides at the stomium level (Fig. 7j).

Pollen grain viability and *in vitro* germination

Pollen stainability, used here as an indirect estimate of viability, remained high in both treatments but decreased slightly under flooding stress (Fig. 8a). Because macrograins containing cytoplasm were scored as stainable, this assay may overestimate functional viability (Fig. 8b). Control plants showed 98.61±0.14% stainable pollen, whereas flooded plants showed 97.03±0.38% ($p < 0.001$), a decrease of 1.58 percentage points in stainability. *In vitro* germination assays demonstrated a significant impairment in pollen tube emergence capacity (Fig. 8c). Mature pollen grains from control plants achieved a germination rate of 60.28±3.19%. In contrast, flooding stress significantly reduced pollen germination to 49.54±3.28% ($p<0.05$). This reduction was accompanied by the presence of small and empty pollen grains (Fig. 8d). The observed macrograins were classified as abnormal due to non-germination or the formation of abnormal short pollen tubes (Fig. 8e).

Discussion

This study revealed that flooding induced cytological, histological, and developmental abnormalities in *S. lycopersicum* cv. Ailsa Craig. The observed effects followed a developmental stage-specific pattern and, taken together, affected the male reproductive performance. During meiosis, the flooding shifted the distribution of meiocytes towards later developmental stages and increased the frequencies of some abnormalities, triggering triad formation. Anatomically, flowers that developed at the end of the flooding treatment exhibited alterations in tapetum development and, in some cases, degeneration of microspore mother cells (MMCs). In post-meiotic floral buds, male gametogenesis was more developmentally advanced than in controls at comparable bud sizes. Finally, *in vitro* germination assays demonstrated a significant reduction in pollen germination.

Microsporogenesis and microgametogenesis are central to plant reproduction (Begcy et al. 2024; Qian et al. 2025). Successful male gamete development is essential for seed production in many crops. Failures during meiosis can lead to pollen sterility and reduced seed set (Qian et al. 2025). Such sensitivity of the reproductive tissue to environmental extremes can compromise reproductive success and crop yield (Ganie and Foyer 2023; Begcy et al. 2024). Our data showed that tomato male meiosis is particularly sensitive to abiotic stress; analysis of meiotic stage distribution demonstrated that flooding shifted meiocytes towards later stages of meiosis: control plants had a higher frequency of cells in prophase I, whereas flooded plants had a higher proportion reaching telophase II (Fig. 2p). This shifting effect towards later stages was supported by the weighted means of meiosis stages (Table 1). Temperature stress is known to alter the duration of meiosis and pollen maturation in cereals; Bennett et al. (1972), for example, showed progressively shorter meiotic and pollen-development durations in wheat and rye as growth temperature increased from 15 to 25 °C, and Wilson (1959) also demonstrated a temperature dependence of meiotic duration. Recent work has emphasised that environmental

conditions and genotype can alter the timing of male gametophyte development and complicate developmental-stage prediction (Masoomi-Aladizgeh et al. 2025). However, because the present experiment assessed meiotic stages at a single sampling time, the higher progression indices should be interpreted as a shift in stage distribution rather than direct evidence that flooding accelerates the meiotic process. Future studies should explore meiotic rate dynamics by incorporating additional time-resolved measurements.

Tomato plants subjected to simulated flooding exhibited abnormal meiotic behavior, including chromosome bridges, laggards, asynchrony, and trinuclear meiocytes. While the first meiotic division displayed lower frequencies of laggards and bridges, the second division showed higher instability, characterized by bridges, laggards, asynchrony, and the formation of trinuclear meiocytes. These findings indicate that the second meiotic division is particularly sensitive to flooding stress, representing a vulnerable stage during male meiosis. In a comparable approach, Schindfessel et al. (2023) exposed 'Micro-Tom' tomatoes to short-term heat stress to simulate the effect of heat waves during microsporogenesis. Notably, they found that Meiosis I (specifically anaphase I) was the most vulnerable phase under heat stress, exhibiting the highest frequency of meiotic irregularities. This contrast suggests that the vulnerability of the different meiotic stages vary in relation to the specific nature of the abiotic stressor. Given that hormonal interactions and DNA repair mechanisms are stress-specific, further investigation into the physiological responses of reproductive tissues during flooding is warranted. To date, this is the first study to comprehensively evaluate the impact of flooding across male gametophyte development in tomatoes, laying the groundwork for future physiological studies.

Meiosis is a highly conserved process among eukaryotes which involves a single replication phase followed by two consecutive steps of chromosome segregation (Mercier et al. 2015). Precise functional synchronization of the stages, called meiotic synchrony, ensures proper chromosome pairing and segregation, yielding fertile reduced male gametes (Magnard et al. 2001; Zamariola et al. 2014). The opposite, meiotic asynchrony, characterised by chromosome asynapsis and unbalanced segregation, leads to unreduced male gametes and sterile pollen grains (Carrizo García et al. 2017; Schindfessel et al. 2023). Cytogenetic analysis revealed that meiotic asynchrony was the most frequent abnormality in both treatments, reaching its highest frequency under flooding. This phenomenon was detected during metaphase and anaphase of the second meiosis: in the first only one nucleus enters metaphase II, while the other nucleus remains in prophase II; the second meiotic asynchrony observed is characterised by the presence of one nucleus in metaphase and the other nucleus with its chromosomes already segregating to the poles. The result are gametes with unreduced diploid chromosome number, which is confirmed by the significant observed increase of trinuclear configurations at telophase II. This abnormality, commonly observed in tomatoes under heat stress (Schindfessel et al. 2023), has now been documented under flooding stress as well. Abnormal spindle orientation, meiotic restitution, and

defective cytokinesis are recognised mechanisms that can generate abnormal sporads and, in some cases, unreduced (2n) gametes (Bretagnolle and Thompson 1995; De Storme and Geelen 2013). In the case of short-term heat stress, cytokinesis and meiotic progression is disrupted producing restitutional meiotic products in barley and tomato (Schindfessel et al. 2021, 2023). Our findings shed light on the meiotic behaviour under short-term flooding and suggest that flooding stress can disrupt meiotic progression and cytokinesis in tomato, potentially increasing the occurrence of unreduced gametes.

Overall, these observations provide a plausible cytological framework for interpreting male meiotic responses to flooding in tomato. Flooding did not cause a generalised collapse of meiosis; rather, it was associated with a shift towards later meiotic stages, a numerically higher frequency of meiotic asynchrony and trinuclear configurations at telophase II, followed by a significant reduction in normal tetrads and an increase in triads. Because normal tetrads still represented more than 94% of the sporads under flooding, this pattern is better interpreted as a modest but significant disruption of sporad formation rather than a large loss of normal sporads. Moreover, most individual chromosome abnormalities did not differ significantly between treatments. Together, these results suggest that the meiocytes derived from Meiosis I entering Meiosis II, are specially vulnerable to six-day of hypoxia.

Stainability and *in vitro* germination provide complementary, but not equivalent, estimates of pollen viability and function (Dafni and Firmage 2000). After six days of flooding, pollen stainability remained very high and declined by only 1.58 percentage points, whereas *in vitro* germination decreased from 60.28% to 49.54%, corresponding to an approximately 18% relative reduction. This contrast suggests that the carmine:glycerine assay largely reflected cytoplasmic integrity, whereas germination provided a more stringent measure of functional pollen performance under flooding. Environmental stress can affect pollen number, viability, germination, pollen-tube growth and biochemical composition, but flooding has received considerably less attention than heat and drought in this context (Althiab-Almasaud et al. 2024). In *Clivia miniata*, flooding reduced pollen quantity and quality, with the number of pollen grains per anther showing the greatest sensitivity, followed by pollen germination and fertility (Yamburov et al. 2014). A comparable sensitivity of functional pollen traits is observed under heat stress in tomato: exposure to 32/26 °C reduces both pollen release and germination (Sato and Peet 2005). Exposure of tomato ‘Micro-Tom’ plants to short periods of high temperature during microsporogenesis accelerates pollen senescence, drastically shortening gametophyte lifespan and ultimately resulting in complete loss of pollen viability (Iovane and Aronne 2022). In contrast, the present results indicate that flooding stress, although detrimental to male reproductive development, had a less severe effect on pollen viability than high-temperature stress. This difference highlights the particularly high sensitivity of tomato pollen development to elevated temperature, which can severely disrupt reproductive processes and compromise pollen function. Comparable detrimental effects of heat stress on reproductive development and pollen performance have been documented in several other crop species

(Porch and Jahn 2001; Giorno et al. 2013; Jagadish et al. 2014; Masoomi-Aladizgeh et al. 2020). The pronounced effects of heat stress on male reproductive function may therefore explain the greater attention it has received compared with flooding, while also underscoring the need for further research into the consequences of flooding stress in tomato reproductive fitness.

Abiotic stress can perturb reactive oxygen species (ROS) homeostasis and carbohydrate metabolism during pollen development, with consequences for pollen survival, wall integrity, germination and pollen-tube growth (Muhlemann et al. 2018; Chaturvedi et al. 2021; Xie et al. 2022; Ali and Muday 2024). In tomato, Pressman et al. (2002) associated heat-induced reductions in pollen viability with altered carbohydrate concentrations in developing anthers, particularly during the sensitive period preceding anthesis. These mechanisms provide plausible context for the reduced pollen germination observed here, although ROS status and carbohydrate metabolism were not measured in the present flooding experiment.

Histological analysis further suggests that the reduction in pollen performance may be associated with developmental alterations in anther tissues, particularly the tapetum. The tapetum supplies nutrients and enzymes to developing microspores and contributes essential materials for pollen-wall formation (Pacini et al. 1985; Ferguson et al. 2017). Its degeneration is controlled by a tightly regulated programme of cell death, and disruption of the timing of this process can compromise microspore development and male fertility (Papini et al. 1999; Parish and Li 2010; Wei and Ma 2023). Abiotic stresses can perturb tapetal development in different ways (Parish et al. 2012). In tomato, moderately elevated temperature delayed tapetal degradation (Sato et al. 2006), whereas exposure to 36/26 °C caused marked degeneration of tapetal cells and microspores (Giorno et al. 2013). Drought also causes stage-specific abnormalities in tomato anthers and pollen, with the tetrad-to-vacuolated uninucleate microspore stages being particularly sensitive (Lamin-Samu et al. 2021). In the present study, the occurrence of degenerating tapetal cells in some locules and enlarged or persistent tapetal cells in others suggests a heterogeneous disturbance of tapetal development. These observations are consistent with a disturbance in the timing of tapetal degeneration. Because PCD markers were not directly assessed, however, the histological changes should be interpreted as altered tapetal degeneration rather than direct evidence of premature or delayed PCD. ROS homeostasis is closely associated with the initiation and progression of tapetal PCD in tobacco and tomato, and experimental perturbation of ROS levels impairs pollen development (Yu et al. 2017). Ethylene is another plausible candidate signal under flooding. In *Arabidopsis*, excessive ethylene signalling through the EIN2-EIN3/EIL1 pathway induces premature tapetal degeneration and impairs microspore development (Zhu et al. 2022). In flooded tomato, ethylene signalling is a major component of the adaptive response and contributes to adventitious-root and aerenchyma-related responses in submerged tissues (Vidoz et al. 2010; Mignolli et al. 2020). Although a direct involvement of ethylene or ROS in the anther alterations observed here remains to be

demonstrated, these pathways provide testable hypotheses for future studies of flooding-induced disruption of tapetal development.

The marked alterations observed in early flower buds (3–5 mm) after six days of flooding indicate that these developmental stages are particularly responsive to root hypoxia. Longer or more severe flooding could plausibly intensify these effects, but this possibility requires new direct experimental testing. Drought stress in tomato likewise causes stage-specific anther failure, pollen abortion, inadequate starch accumulation and anther indehiscence, with the tetrad-to-vacuolated uninucleate microspore stages showing particularly high sensitivity (Lamin-Samu et al. 2021). Thus, distinct water-related stresses can converge on vulnerable phases of anther and pollen development, although the underlying mechanisms may differ. Overall, the observed differences in microsporogenesis, tapetal development and *in vitro* pollen germination suggest that male reproductive development in tomato is sensitive to flooding. Further experiments on female development are needed in order to provide a general framework for investigating the physiological and signalling mechanisms linking hypoxia stress to fertilization, seed set production and fruit quality.

Acknowledgements

We are grateful for the postdoctoral fellowship awarded to Y.J.P. by the Consejo Nacional de Investigaciones Científicas y Técnicas.

Funding

This work was supported by the Consejo Nacional de Investigaciones Científicas y Técnicas (PIP 11220220100567CO) and by Secretaría General de Ciencia y Técnica (Universidad Nacional del Nordeste) PINOV 24PN01.

Author contributions

Y.J.P. performed the experimental work, collected and performed the histological preparations, analyzed, interpreted and photographed the cytogenetics results, wrote the original draft, prepared the figures; L.M.Z. helped to collect the material and performed the histological preparations, analyzed, interpreted and photographed the anatomical results, helped to write the original draft; F.M. performed the statistical analysis, helped to interpret the results, contributed to the discussions, reviewed and collaborated in the drafting of the manuscript; S.S. helped with pollen tests and experimental work; A.M.G. helped to interpret the results, contributed to the discussions, reviewed and collaborated in the drafting of the manuscript; M.L.V. designed the experimental work, contributed to the discussions, reviewed and collaborated in the drafting of the manuscript.

Data availability statement

All data generated or analyzed during this study are included within this article.

Disclosure statement

The authors report there are no competing interests to declare.

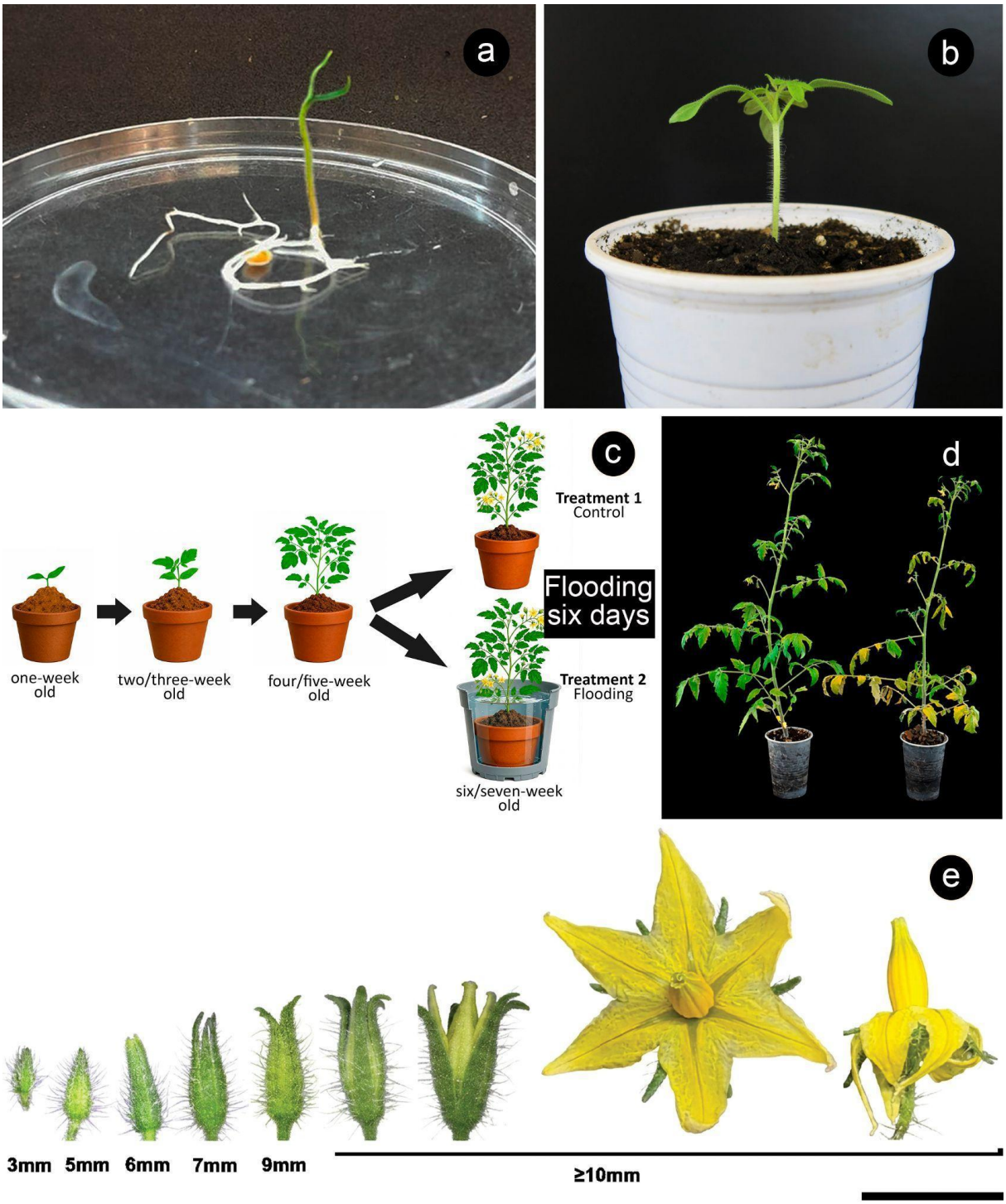


Fig. 1 Growing and handling of *Solanum lycopersicum* cv. Ailsa Craig. **a** One-week-old plant. **b,** Transplanted two-week-old plant. **c** Experimental design. **d** Seven-week-old plants after treatments. **e** Flower stages analysed in both treatments: flower buds 3–5 mm long, with closed calyx; flower buds 6–9 mm long, with open calyx

but closed corolla; flowers ≥10 mm long, corresponding to anthesis, when the corolla emerges from the sepals, expands fully to expose the anther cone, and recurves. Scale bar: 10 mm

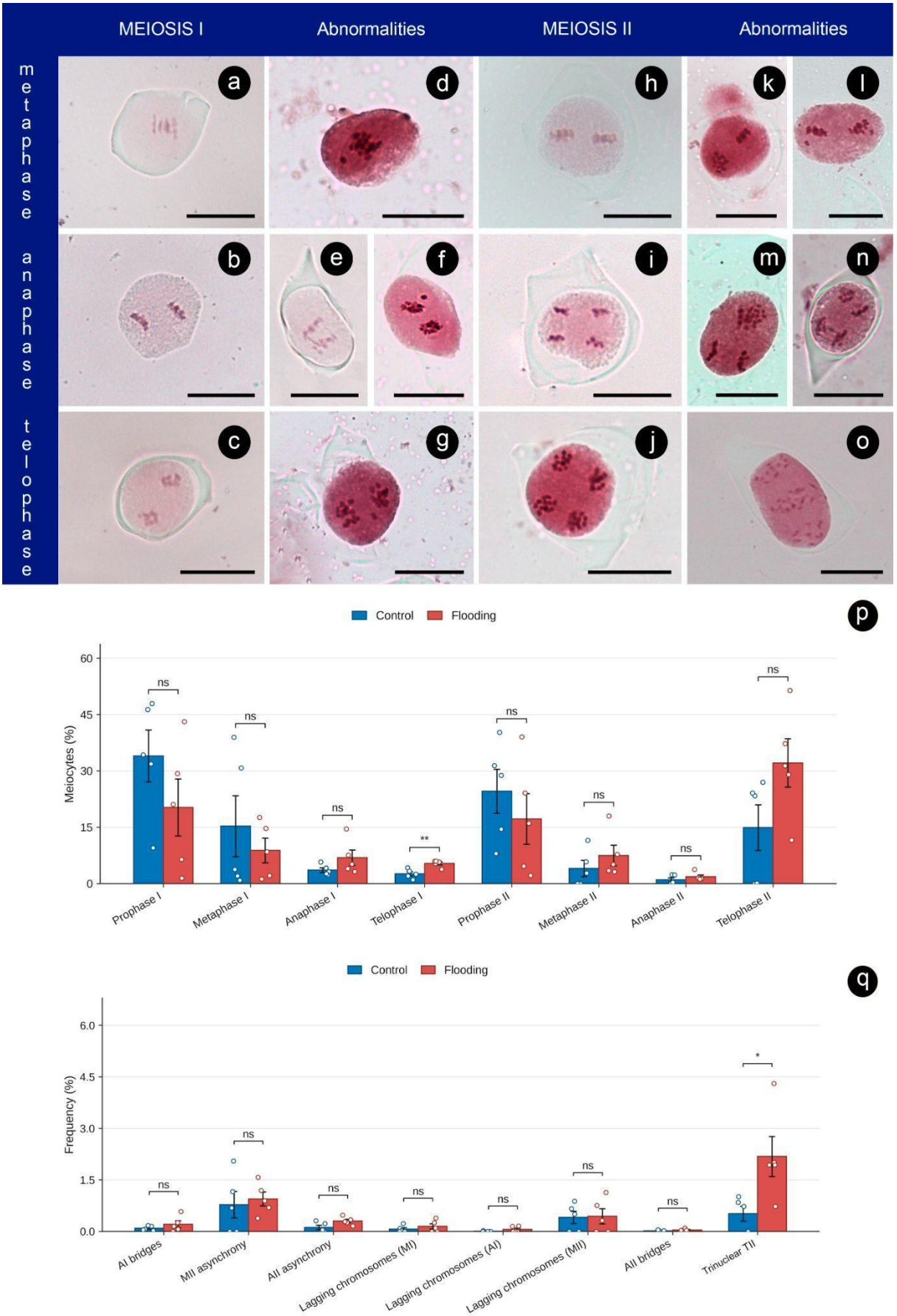


Fig. 2 Meiotic phases and their observed abnormalities during microsporogenesis, along with corresponding

quantitative analyses in *Solanum lycopersicum* cv. Ailsa Craig under control and flooding conditions. **a–c** Normal Meiosis I. **d–g** Abnormalities observed during Meiosis I. **d** Laggard at metaphase I. **e** Bridge at anaphase I. **f** Laggard at anaphase I. **g** Laggard at late telophase I. **h–j** Normal Meiosis II. **k–o** Abnormalities observed during Meiosis II. **k** asynchrony at metaphase II. **l** Laggards in metaphase II. **m** Asynchrony in anaphase II. **n** Bridges at anaphase II. **o** Trinuclear meiocyte. **p** Frequencies (%) of microsporocytes at different meiotic phases in control (blue) and flooded (orange) plants. Bars display mean values ± SEM, and individual dots represent biological replicates. Normality and homoscedasticity were verified using Shapiro–Wilk and Levene's tests, followed by Student's t-test, Welch's t-test, or Mann–Whitney U test according to data distribution. ns, not significant; **p<0.01. **q** Frequency (%) of microsporocytes exhibiting meiotic abnormalities in control (blue) and flooded (orange) plants. Bars show mean values ± SEM, and individual dots represent the biological replicates. Normality and variance homogeneity were verified using the Shapiro–Wilk and Levene's tests, followed by Student's t-test, Welch's t-test, or Mann–Whitney U test, depending on the data distribution. ns, not significant; *p<0.05. Scale bars: a-o=20 µm

Table 1. Effect of flooding on meiotic progression. Values are means ± SEM of five biological replicates. Weighted mean meiotic stage values (WMMS-I and WMMS-II) range from 1 to 4, with higher values indicating that the meiocyte population is distributed toward later stages of the respective meiotic division. Differences between control and flooded plants were evaluated using an exact one-sided Mann–Whitney U test. Significant differences ($P < 0.05$) are shown in bold.

Meiotic progression index	**Control**	**Flooding**	**P-value**
WMMS-I	1.60 ± 0.14	**1.99 ± 0.21**	**0.048**
WMMS-II	1.77 ± 0.31	**2.85 ± 0.34**	**0.028**

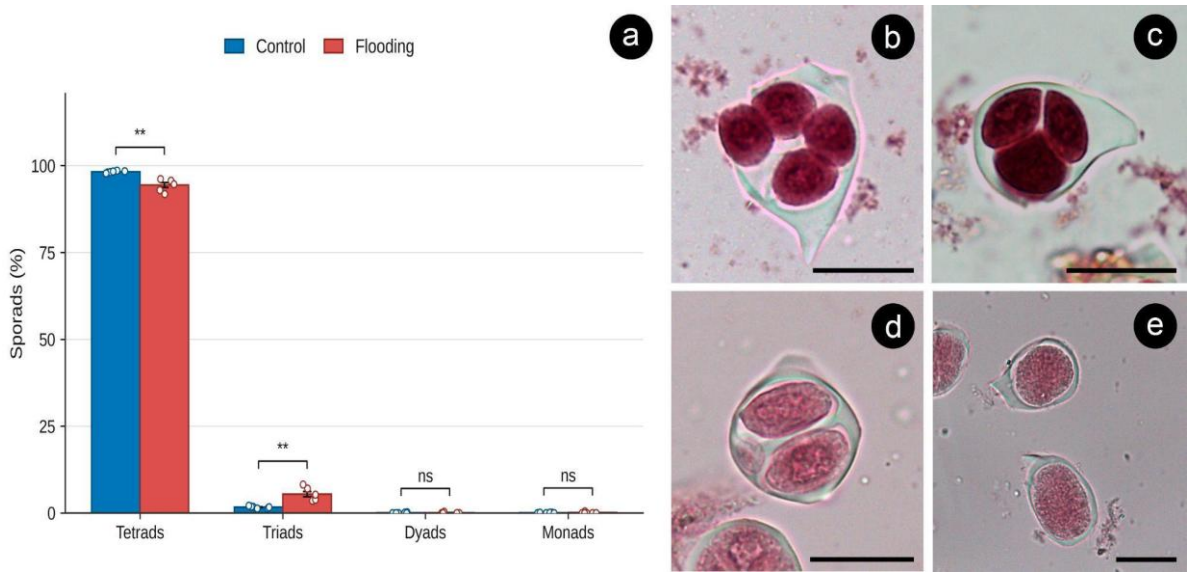


Fig. 3 Effect of flooding stress on sporad configuration in *Solanum lycopersicum* cv. Ailsa Craig. **a** Proportions of normal tetrads and other observed sporad configurations (triads, dyads, and monads) in control (blue) and flooded (orange) plants. Bars represent

mean ± SEM; gray points indicate individual biological replicates. Significance was determined using Shapiro–Wilk and Levene's tests followed by Student's t-test, Welch's t-test, or Mann–Whitney U test as appropriate. ns=not significant, $**p<0.01$. **b** Normal tetrad. **c–e** Abnormal configurations. **c** Triad. **d** Dyad. **e** Monad. Scale bars: **b–e**=20 μm

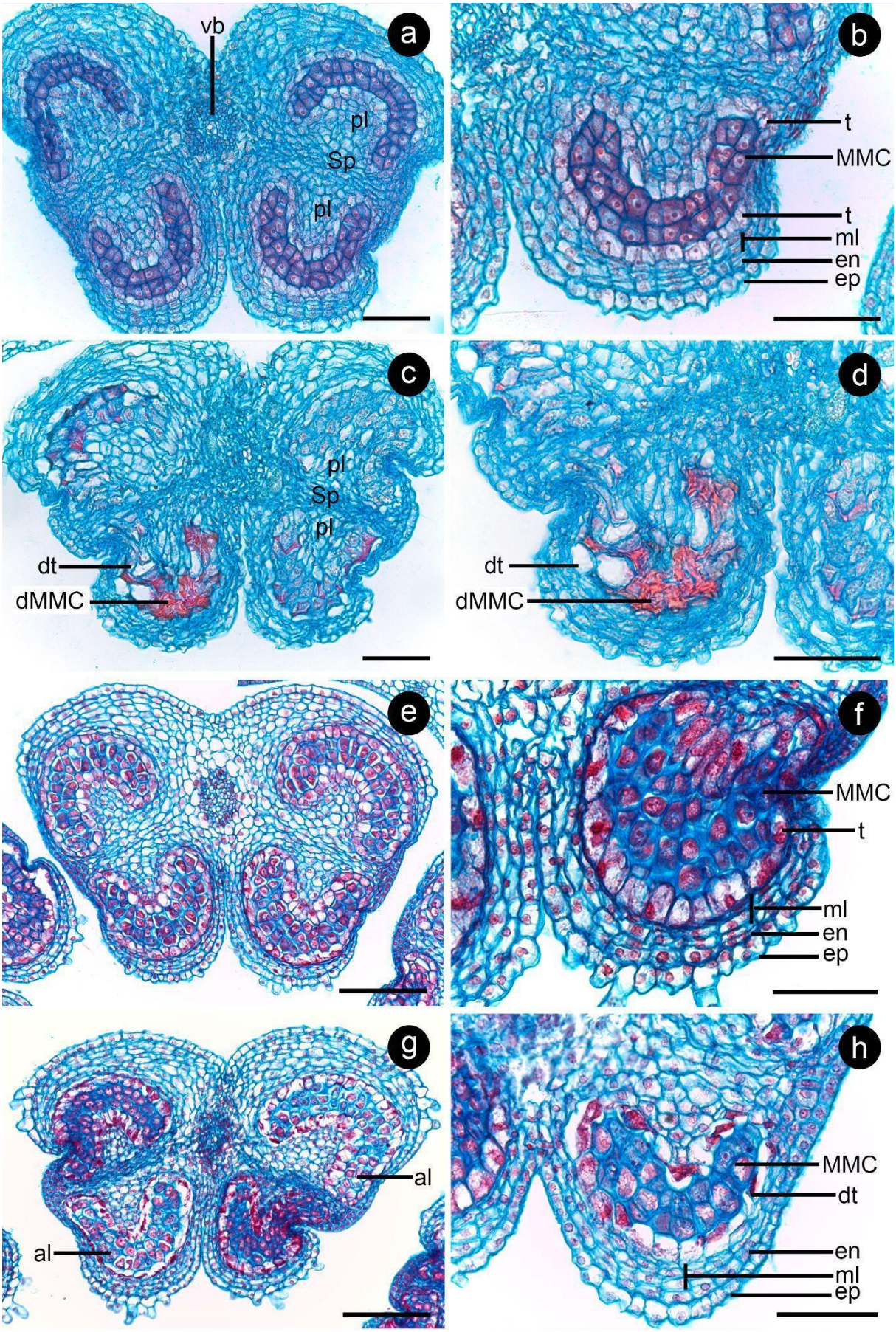


Fig. 4 Anther development in *S. lycopersicum* cv. Ailsa Craig. Floral stages 3 mm (**a–d**) and 4 mm (**e–h**). **a, b, e,**

f Anthers under control conditions. **c, d, g, h** Histological alterations under flooding conditions. **a–h** Microspore mother cell stage. **a–d** Early stage of microspore mother cell differentiation. **e–h** Later stages of microspore mother cells. Abbreviations: al: aborted locule; dMMC: degenerated microspore mother cell; dt: degenerated tapetum; en: endothecium; ep: epidermis; ml: middle layer; MMC: microspore mother cell; pl: placentoid; sp: septum; t: tapetum; vb: vascular bundle. Scale bars: **a, c, e, g,** 100 μm; **b, d, f, h,** 50 μm

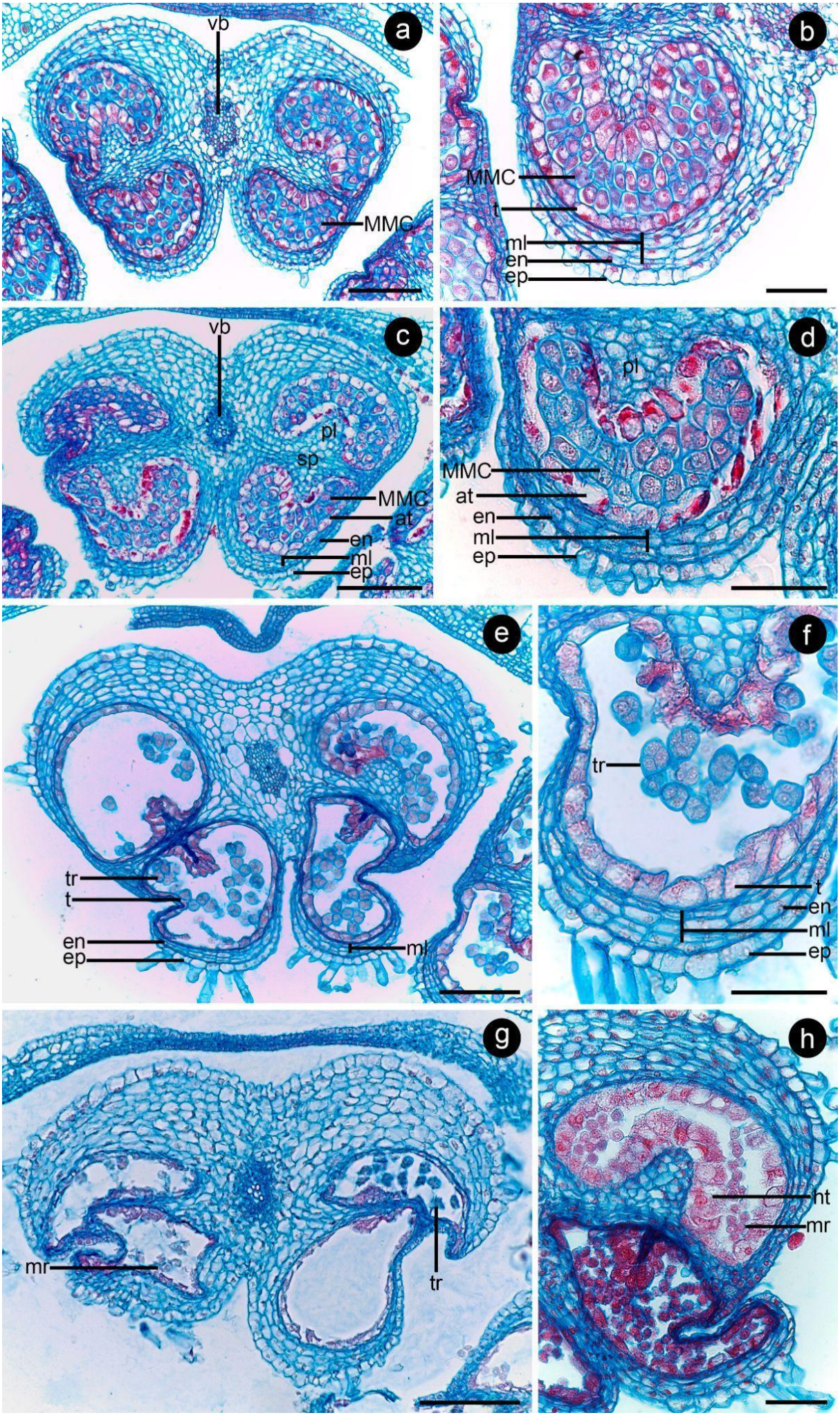

a
vb
MMC
b
MMC
t
ml
en
ep
c
vb
pl
sp
MMC
at
en
ml
ep
d
pl
MMC
at
en
ml
ep
e
tr
t
en
ep
ml
f
tr
t
en
ml
ep
g
mr
tr
h
ht
mr

Fig. 5 Anther development in *S. lycopersicum* cv. Ailsa Craig. 5 mm floral bud stage. **a, b, e, f** Anthers under control conditions; **c, d, g, h** Histological alterations in anthers developing under flooding conditions. **a–d** Microspore mother cell stage. **e, f** Tetrad of microspores stage. **g** Tetrad and early free microspore stages within the same anther. **h** Early free microspore stage. Abbreviations: at: aborted tapetum; en: endothecium; ep: epidermis; ml: middle layer; MMC: microspore mother cell; mr: microspore; pl: placentoid; sp: septum; t: tapetum; tr: tetrad; vb: vascular bundle. Scale bars: **a, c, e, g,** 100 μm; **b, d, f, h,** 50 μm

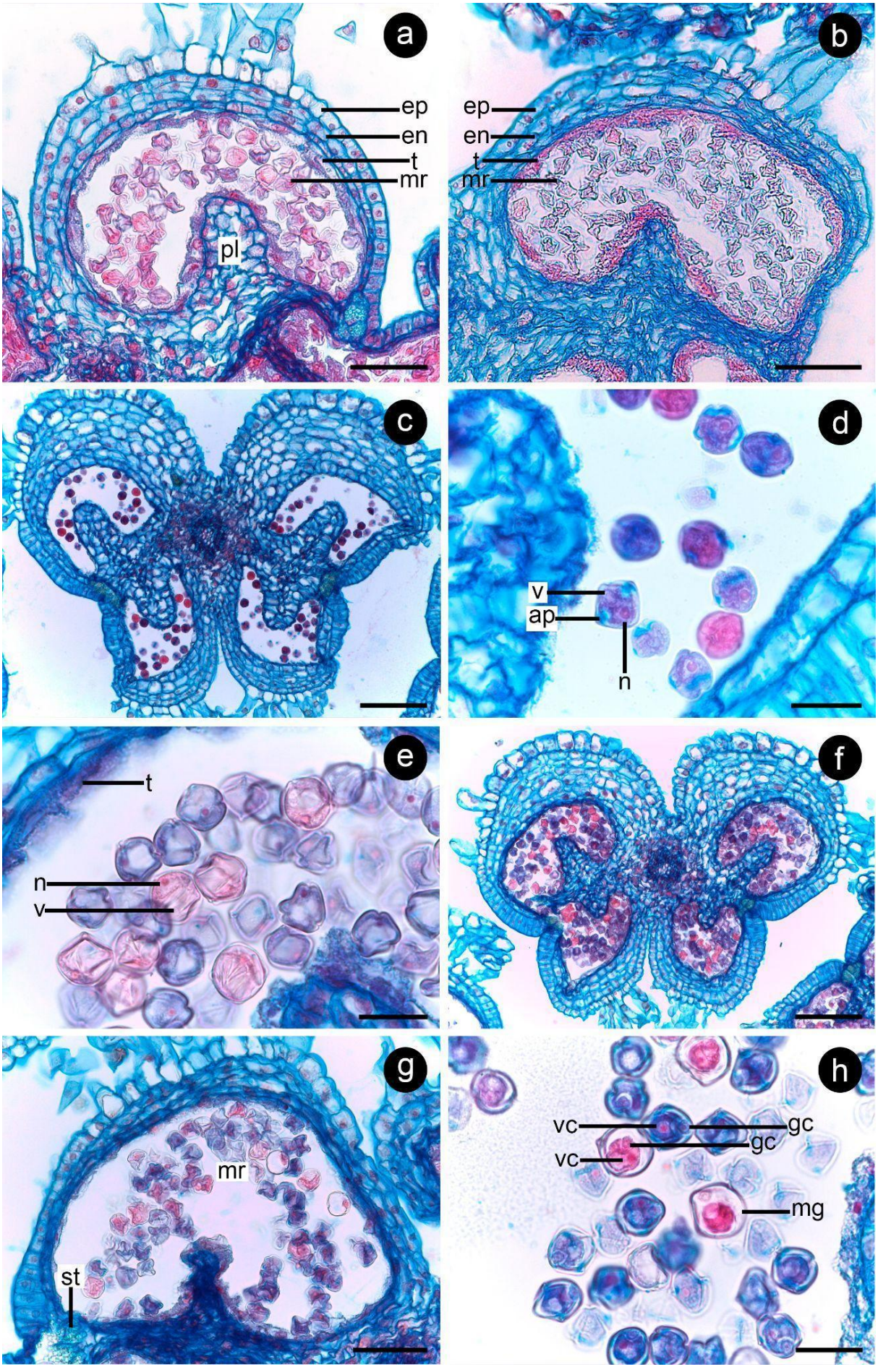

a
ep
en
t
mr
pl
b
ep
en
t
mr
c
d
v
ap
n
e
t
n
v
f
g
mr
st
h
vc
gc
gc
vc
mg

Fig. 6 Anther development in *S. lycopersicum* cv. Ailsa Craig. Floral stages 6 mm (**a, b**) and 7 mm (**c–h**). **a, c–e** Anthers under control conditions; **b, f–h** Anthers under flooding conditions. **a, b** Early and mid-microspore stages. **c–f** Mid- and late microspore stages. **g, h** Young bicellular pollen stage. Abbreviations: ap: pollen aperture; en: endothecium; ep: epidermis; gc: generative cell; mg: macrograin; mr: microspores; n: nucleus; pl: placentoid; sp: septum; t: tapetum; v: vacuole; vc: vegetative cell. Scale bars: **a, b, g,** 50 µm; **c, f,** 100 µm; **d, e, h,** 20 µm

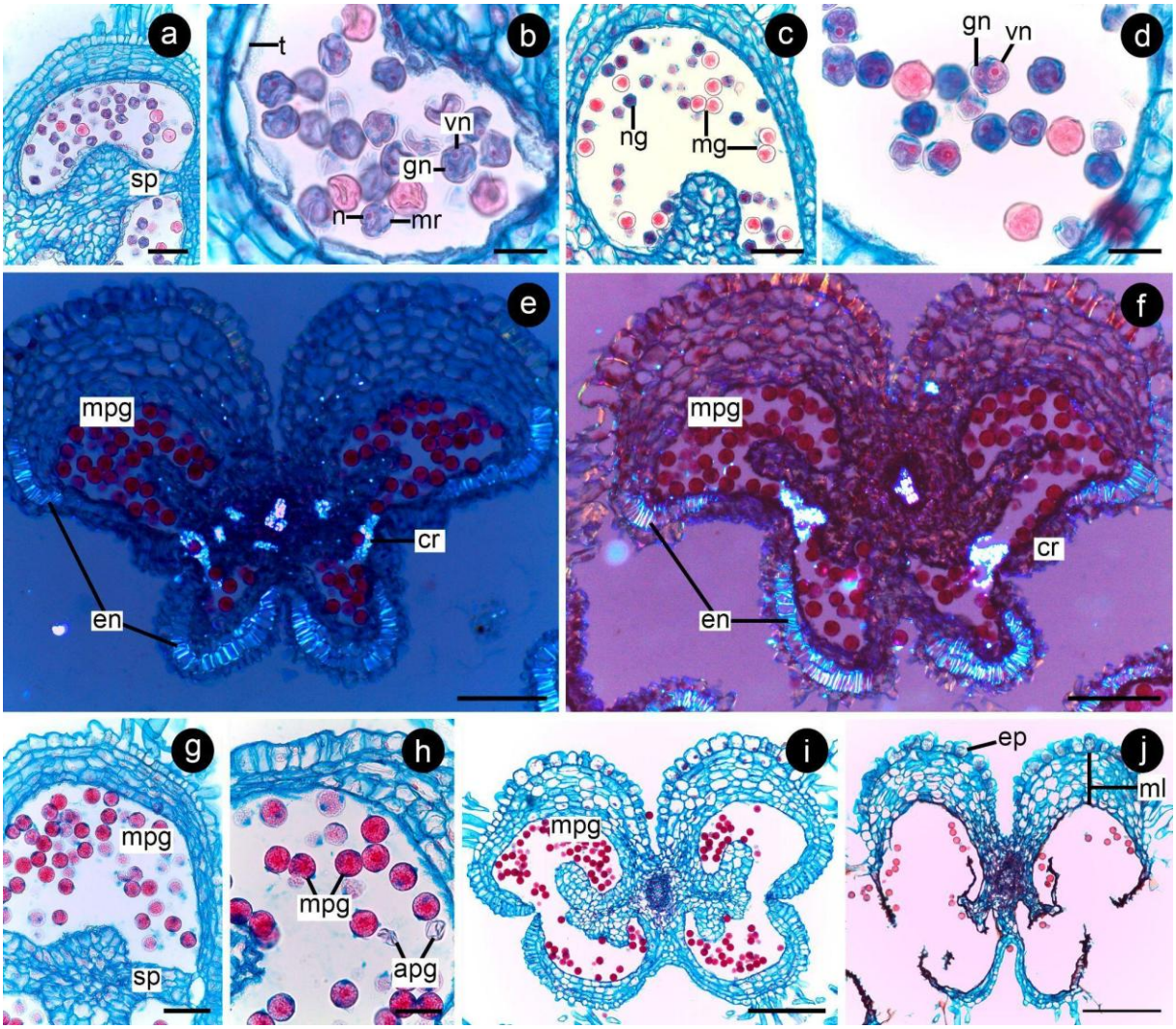


Fig. 7 Anther development in *S. lycopersicum* cv. Ailsa Craig. Floral stages 8 (**a–e**), 9 (**f–h**), and ≥10 mm (**i, j**). **a, b, e, g, i** Anthers under control conditions; **c, d, f, h, j** Anthers under flooding treatment. **a–d** Young pollen grain stage. **e, f** Endothecium secondary wall thickenings under polarised light. **g, h** Mature bicellular pollen grain stage. **i, j** Anther dehiscence. Abbreviations: apg: aborted pollen grain; cr: crystals of calcium oxalate; en: endothecium; ep: epidermis; gn: generative nucleus; mg: macrograin; ml: middle layers; mr: microspore; mpg: mature pollen grain; n: nucleus; ng: normal pollen grain; sp: septum; t: tapetum; vn: vegetative nucleus. Scale bars: **i, j**=200 µm; **e, f**= 100 µm; **a, c, g**= 50 µm; **b, d, h**=20 µm

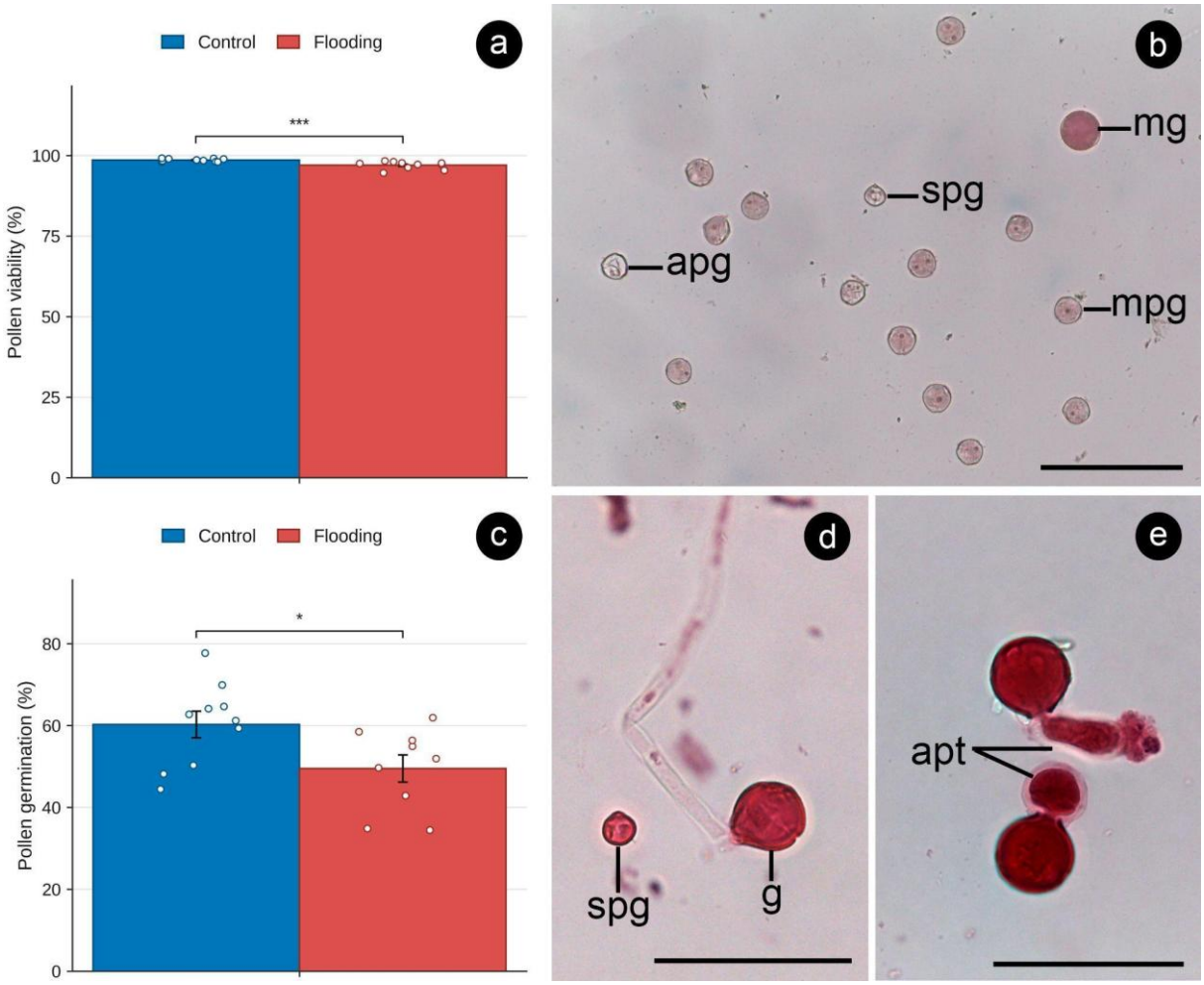


Fig. 8 Pollen viability and in vitro germination test of flooded and control tomato (*S. lycopersicum* cv. Ailsa Craig). **a** Percentage of viable pollen grains in control (blue) and flooded (red) tomato flowers. Bars represent mean ± SEM; gray points represent individual biological replicates. ***p<0.001. **b** Different types of pollen grains observed during the pollen viability test. **c** Percentage of germinated pollen grains under control and flooded conditions. Bars represent mean ± SEM; gray points represent individual biological replicates. *p<0.05. **d** Germinated pollen grains (g) and non-germinated pollen grains (spg). **e** Macrograins with abnormal pollen tube development (apt). Abbreviations: apg: aborted pollen grain; apt: abnormal pollen tube; g: germinated pollen grain; mg: macrograin; mpg: mature pollen grain; spg: small pollen grain. Scale bars: **b** = 100 µm; **d, e** = 50 µm

References

Ali MF, Muday GK (2024) Reactive oxygen species are signaling molecules that modulate plant reproduction. Plant Cell Environ 47:1592-1605. https://doi.org/10.1111/pce.14837

Althiab-Almasaud R, Teyssier E, Chervin C, Johnson MA, Mollet JC (2024) Pollen viability, longevity, and function in angiosperms: key drivers and prospects for improvement. Plant Reprod 37:273-293. https://doi.org/10.1007/s00497-023-00484-5

Begcy K, Mendes MA, De Storme N (2024) Plant reproduction under environmental stress. Front Plant Sci 15:1369070. https://doi.org/10.3389/fpls.2024.1369070

Beisken S, Earll M, Baxter C, Portwood D, Ament Z, Kende A et al (2014) Metabolic differences in ripening of *Solanum lycopersicum* 'Ailsa Craig' and three monogenic mutants. Sci Data 1:140029. https://doi.org/10.1038/sdata.2014.29

Bennett MD, Smith JB, Kemble R (1972) The effect of temperature on meiosis and pollen development in wheat and rye. Can J Genet Cytol 14:615-624. https://doi.org/10.1139/g72-076

Bretagnolle F, Thompson JD (1995) Gametes with the somatic chromosome number: mechanisms of their formation and role in the evolution of autopolyploid plants. New Phytol 129:1-22. https://doi.org/10.1111/j.1469-8137.1995.tb03005.x

Brewbaker JL, Kwack BH (1963) The essential role of calcium ion in pollen germination and pollen tube growth. Am J Bot 50:859-865. https://doi.org/10.1002/j.1537-2197.1963.tb06564.x

Carrizo García C, Nepi M, Pacini E (2017). It is a matter of timing: asynchrony during pollen development and its consequences on pollen performance in angiosperms—a review: CC García et al. Protoplasma 254(1):57-73. https://doi.org/10.1007/s00709-016-0950-6

Chaturvedi P, Wiese AJ, Ghatak A, Zaveska Drabkova L, Weckwerth W, Honys D (2021) Heat stress response mechanisms in pollen development. New Phytol 231:571-585. https://doi.org/10.1111/nph.17380

Choudhary M, Yan G, Siddique KHM, Cowling WA (2022) Heat stress during meiosis has lasting impacts on plant growth and reproduction in wheat (*Triticum aestivum* L.). Agronomy 12:987. https://doi.org/10.3390/agronomy12050987

Dafni A, Firmage D (2000) Pollen viability and longevity: practical, ecological and evolutionary implications. Plant Syst Evol 222:113-132. https://doi.org/10.1007/BF00984098

Darby LA, Ritchie DB, Taylor IB (1978) Isogenic lines of the tomato 'Ailsa Craig'. Annu Rep Glasshouse Crops Res Inst, pp 168-184.

De Pedro LF, Mignolli F, Scartazza A, Melana Colavita JP, Bouzo CA, Vidoz ML (2020) Maintenance of photosynthetic capacity in flooded tomato plants with reduced ethylene sensitivity. Physiol Plant 170:202-217. https://doi.org/10.1111/ppl.13141

De Storme N, Geelen D (2013) Sexual polyploidization in plants - cytological mechanisms and molecular regulation. New Phytol 198:670-684. https://doi.org/10.1111/nph.12184

Dyer AF (1963) The use of lacto-propionic orcein in rapid squash methods for chromosome preparations. Stain Technol 38:85-90. https://doi.org/10.3109/10520296309061169

Else MA, Janowiak F, Atkinson CJ, Jackson MB (2009) Root signals and stomatal closure in relation to photosynthesis, chlorophyll a fluorescence and adventitious rooting of flooded tomato plants. Ann Bot 103:313-323. https://doi.org/10.1093/aob/mcn208

Ezin V, Pena RDL, Ahanchede A (2010) Flooding tolerance of tomato genotypes during vegetative and reproductive stages. Braz J Plant Physiol 22:131-142. https://doi.org/10.1590/S1677-04202010000200007

Ferguson AC, Pearce S, Band LR, Yang C, Ferjentsikova I, King J et al (2017) Biphasic regulation of the transcription factor ABORTED MICROSPORES (AMS) is essential for tapetum and pollen development in Arabidopsis. New Phytol 213:778-790. https://doi.org/10.1111/nph.14200

Fernández A (1973) El ácido láctico como fijador cromosómico. Bol Soc Argent Bot 15:287-290.

Ganie SA, Foyer CH (2023) Environmental stress in crops: effects and responses during reproduction. Food Energy Secur 12:e515. https://doi.org/10.1002/fes3.515

Germain V, Ricard B, Raymond P, Saglio PH (1997) The role of sugars, hexokinase, and sucrose synthase in the determination of hypoxically induced tolerance to anoxia in tomato roots. Plant Physiol 114:167-175. https://doi.org/10.1104/pp.114.1.167

Giorno F, Wolters-Arts M, Mariani C, Rieu I (2013) Ensuring reproduction at high temperatures: the heat stress response during anther and pollen development. Plants 2:489-506. https://doi.org/10.3390/plants2030489

González AM, Cristóbal CL (1997) Anatomía y ontogenia de semillas de *Helicteres lhotzkyana* (Sterculiaceae). Bonplandia 9:287-294. https://doi.org/10.30972/bon.93-41497

Horchani F, Aloui A, Brouquisse R, Aschi-Smiti S (2008) Physiological responses of tomato plants (*Solanum lycopersicum*) as affected by root hypoxia. J Agron Crop Sci 194:297-303. https://doi.org/10.1111/j.1439-037X.2008.00313.x

Horchani F, Aschi-Smiti S (2011) Prolonged root hypoxia effects on ethylene biosynthesis and perception in tomato fruit. Plant Signal Behav 6:1-4. https://doi.org/10.4161/psb.6.1.13880

Horchani F, Khayati H, Aschi-Smiti S (2011) Contrasted responses to root hypoxia in tomato fruit at two stages of development. J Plant Biol 54:15-22. https://doi.org/10.1007/s12374-010-9137-4

Huang X, Zhang X, Huo Y, Chen D, Zhou Z, Ali S, Zheng G, Peng B, Tang L, Hu W (2023) Different soil moisture induced by groundwater depth alter cotton pollen fertility by affecting anther carbohydrate and antioxidant metabolism and its relationship with cottonseed yield. J Plant Growth Regul 42:3498-3514. https://doi.org/10.1007/s00344-022-10813-z

Iovane M, Aronne G. (2022). High temperatures during microsporogenesis fatally shorten pollen lifespan. Plant Reprod 35(1):9-17. https://doi.org/10.1007/s00497-021-00425-0

Jackson MB, Campbell DJ (1976) Waterlogging and petiole epinasty in tomato: the role of ethylene and low oxygen. New Phytol 76:21-29. https://doi.org/10.1111/j.1469-8137.1976.tb01434.x

Jagadish KS, Craufurd P, Shi W, Oane R (2014) A phenotypic marker for quantifying heat stress impact during microsporogenesis in rice (*Oryza sativa* L.). Funct Plant Biol 41(1):48-55. https://doi.org/10.1071/FP13086

Jegadeesan S, Chaturvedi P, Ghatak A, Pressman E, Meir S, Faigenboim A et al (2018) Proteomics of heat-stress and ethylene-mediated thermotolerance mechanisms in tomato pollen grains. Front Plant Sci 9:1558. https://doi.org/10.3389/fpls.2018.01558

Johansen DA (1940) Plant microtechnique. McGraw-Hill Book Company, New York

Kouchnareva T (2017) Ailsa Craig. Tatiana's TOMATOBase. https://tatianastomatobase.com. Accessed 28 June 2017

Lamin-Samu AT, Farghal M, Ali M, Lu G (2021) Morpho-physiological and transcriptome changes in tomato anthers of different developmental stages under drought stress. Cells 10:1809. https://doi.org/10.3390/cells10071809

Luque RHC, Sousa HC, Kraus JE (1996) Métodos de coloração de Roeser (1972) modificado e Kropp (1972), visando à substituição do azul de Astra por azul de Alcian 8GS ou 8GX. Acta Bot Bras 10:199-212. https://doi.org/10.1590/S0102-33061996000200001

Magnard JL, Yang M, Chen YS, Leary M, McCormick S (2001). The *Arabidopsis* gene tardy asynchronous meiosis is required for the normal pace and synchrony of cell division during male meiosis. Plant physiol, 127(3):1157-1166. https://doi.org/10.1104/pp.010473

Masoomi-Aladizgeh F, Najeeb U, Hamzelou S, Pascovici D, Amirkhani A, Tan DK, Atwell BJ (2020) Pollen development in cotton (*Gossypium hirsutum*) is highly sensitive to heat exposure during the tetrad stage. Plant Cell Environ 42(1):321–336. https://doi.org/10.1111/pce.13908

Masoomi-Aladizgeh F, Atwell BJ, Bokshi AI, Thistlethwaite RJ, Khoddami A, Trethowan R et al (2025) Pinpointing the timing of meiosis: a critical factor in evaluating the impact of abiotic stresses on the fertility of cereal crops. New Phytol 245:1341-1354. https://doi.org/10.1111/nph.20297

Mercier R, Mézard C, Jenczewski E, Macaisne N, Grelon M. (2015) The molecular biology of meiosis in plants. Annu Rev Plant Biol 66(1):297-327. https://doi.org/10.1146/annurev-arplant-050213-035923

Mignolli F, Barone JO, Vidoz ML (2021) Root submergence enhances respiration and sugar accumulation in the stem of flooded tomato plants. Plant Cell Environ 44:3643-3654. https://doi.org/10.1111/pce.14152

Mignolli F, Todaro JS, Vidoz ML (2020) Internal aeration and respiration of submerged tomato hypocotyls are enhanced by ethylene-mediated aerenchyma formation and hypertrophy. Physiol Plant 169:49-63. https://doi.org/10.1111/ppl.13044

Muhlemann JK, Younts TLB, Muday GK (2018) Flavonols control pollen tube growth and integrity by regulating ROS homeostasis during high-temperature stress. Proc Natl Acad Sci USA 115:E11188-E11197. https://doi.org/10.1073/pnas.1811492115

Neijzing, M.G. & Viegas, W.S. (1979). The effect of rye B-chromosomes on meiotic stability of rye-wheat hybrids in normal, nulli 5B and nulli 5D background. *Genetica* 51: 21–26. https://doi.org/10.1007/BF00139494

Nikolova V, Ganeva D, Stefanova Y (2009) Cytological peculiarities in tomato (*Solanum lycopersicum*) nuclear male sterility. Acta Hortic 830:305–312. https://doi.org/10.17660/ActaHortic.2009.830.43

Pacini E, Franchi GG, Hesse M (1985) The tapetum: its form, function, and possible phylogeny in Embryophyta. Plant Syst Evol 149:155-185. https://doi.org/10.1007/BF00983304

Papini A, Mosti S, Brighigna L (1999) Programmed-cell-death events during tapetum development of angiosperms. Protoplasma 207:213-221. https://doi.org/10.1007/BF01283002

Parish RW, Li SF (2010) Death of a tapetum: a programme of developmental altruism. Plant Sci 178:73-89. https://doi.org/10.1016/j.plantsci.2009.11.001

Parish RW, Phan HA, Iacuone S, Li SF (2012) Tapetal development and abiotic stress: a centre of vulnerability. Funct Plant Biol 39:553-559. https://doi.org/10.1071/FP12090

Peet MM, Sato S, Gardner RG (1998) Comparing heat stress effects on male-fertile and male-sterile tomatoes. Plant Cell Environ 21:225-231. https://doi.org/10.1046/j.1365-3040.1998.00281.x

Peters SA, Underwood CJ (2023) Technology-driven approaches for meiosis research in tomato and wild relatives. Plant Reprod 36:97-106. https://doi.org/10.1007/s00497-022-00450-7

Pittenger TH, Frolik EF (1951) Temporary mounts for pollen abortion determinations. Stain Technol 26:181-184. https://doi.org/10.3109/10520295109113205

Porch TG, Jahn M (2001) Effects of high-temperature stress on microsporogenesis in heat-sensitive and heat-tolerant genotypes of *Phaseolus vulgaris*. Plant Cell Environ 24(7):723-731. https://doi.org/10.1046/j.1365-3040.2001.00716.x

Pressman E, Peet MM, Pharr DM (2002) The effect of heat stress on tomato pollen characteristics is associated with changes in carbohydrate concentration in the developing anthers. Ann Bot 90:631-636. https://doi.org/10.1093/aob/mcf240

Qian D, Wang M, Niu Y, Yang Y, Xiang Y (2025) Sexual reproduction in plants under high temperature and drought stress. Cell Rep 44(3):115390. https://doi.org/10.1016/j.celrep.2025.115390

Resentini F, Orozco-Arroyo G, Cucinotta M, Mendes MA (2023) The impact of heat stress in plant reproduction. Front Plant Sci 14:1271644. https://doi.org/10.3389/fpls.2023.1271644

Rick CM, Butler L (1956) Cytogenetics of the tomato. Adv Genet 8:267-382. https://doi.org/10.1016/S0065-2660(08)60504-0

Safavi-Rizi V, Herde M, Stöhr C (2020) Identification of nitric oxide (NO)-responsive genes under hypoxia in tomato (*Solanum lycopersicum* L.) root. Sci Rep 10:16509. https://doi.org/10.1038/s41598-020-73613-z

Sato S, Kamiyama M, Iwata T, Makita N, Furukawa H, Ikeda H (2006) Moderate increase of mean daily temperature adversely affects fruit set of *Lycopersicon esculentum* by disrupting specific physiological processes in male reproductive development. Ann Bot 97:731-738. https://doi.org/10.1093/aob/mcl037

Sato S, Peet MM (2005) Effects of moderately elevated temperature stress on the timing of pollen release and its germination in tomato (*Lycopersicon esculentum* Mill.). J Hortic Sci Biotechnol 80:23-28. https://doi.org/10.1080/14620316.2005.11511885

Schindfessel C, De Storme N, Trinh HK, Geelen D (2023) Asynapsis and meiotic restitution in tomato male meiosis induced by heat stress. Front Plant Sci 14:1210092. https://doi.org/10.3389/fpls.2023.1210092

Schindfessel C, Drozdowska Z, De Mooij L, Geelen D (2021) Loss of obligate crossovers, defective cytokinesis and male sterility in barley caused by short-term heat stress. Plant Reprod 34:243-253. https://doi.org/10.1007/s00497-021-00415-2

Vidoz ML, Loreti E, Mensuali A, Alpi A, Perata P (2010) Hormonal interplay during adventitious root formation in flooded tomato plants. Plant J 63:551-562. https://doi.org/10.1111/j.1365-313X.2010.04262.x

Vidoz ML, Mignolli F, Aispuru HT, Mroginski LA (2016) Rapid formation of adventitious roots and partial ethylene sensitivity result in faster adaptation to flooding in the aerial roots (aer) mutant of tomato. Sci Hortic 201:130-139. https://doi.org/10.1016/j.scienta.2016.01.032

Wei S, Ma L (2023) Comprehensive insight into tapetum-mediated pollen development in *Arabidopsis thaliana*. Cells 12:247. https://doi.org/10.3390/cells12020247

Wilson Y (1959) Duration of meiosis in relation to temperature. Heredity 13:263-267. https://doi.org/10.1038/hdy.1959.29

Xie DL, Zheng XL, Zhou CY, Kanwar MK, Zhou J (2022) Functions of redox signaling in pollen development and stress response. Antioxidants 11:287. https://doi.org/10.3390/antiox11020287

Yamburov MS, Astafurova TP, Zhuk KV, Romanova SB, Smolina VM (2014) The effects of drought and flood stress on pollen quality and quantity in *Clivia miniata* (Lindl.) Bosse (Amaryllidaceae). Biomed Pharmacol J 7:575-580. https://doi.org/10.13005/bpj/526

Yin J, Niu L, Li Y, Song X, Ottosen CO, Wu Z et al (2023) The effects of waterlogging stress on plant morphology, leaf physiology and fruit yield in six tomato genotypes at anthesis stage. Veg Res 3:31. https://doi.org/10.48130/VR-2023-0031

Yu SX, Feng QN, Xie HT, Li S, Zhang Y (2017) Reactive oxygen species mediate tapetal programmed cell death in tobacco and tomato. BMC Plant Biol 17:76. https://doi.org/10.1186/s12870-017-1025-3

Zamariola L, Tiang CL, De Storme N, Pawlowski W, Geelen D (2014). Chromosome segregation in plant meiosis. Front Plant Sci 5:279. https://doi.org/10.3389/fpls.2014.00279

Zhang H, Lang Z, Zhu JK, Wang P (2025) Tackling abiotic stress in plants: recent insights and trends. Stress Biol 5:8. https://doi.org/10.1007/s44154-025-00216-x

Zhu BS, Zhu YX, Zhang YF, Zhong X, Pan KY, Jiang Y, Wen CK, Yang ZN, Yao X (2022) Ethylene activates the EIN2-EIN3/EIL1 signaling pathway in tapetum and disturbs anther development in *Arabidopsis*. Cells 11:3177. https://doi.org/10.3390/cells11193177